

Particle-scale Analysis of Key Technologies on Cut-and-over Tunnel in Slope Engineering

J.H. Yang^{1,*}, S.R. Wang^{2,4}, H.Q. Zhang³ and C. Cao⁵

¹School of Civil Engineering and Architecture, Zhejiang University of Science & Technology, Hangzhou 310023, China

²School of Civil Engineering and Mechanics, Yanshan University, Qinhuangdao 066004, China

³Beijing Civil King Information Technology Corporation, Ltd., Beijing 100048, China

⁴Opening Laboratory for Deep Mine Construction, Henan Polytechnic University, Jiaozuo 454003, China

⁵Engineering Faculty, University of Wollongong, NSW 2530, Australia

Received 29 March 2014; Accepted 15 August 2014

Abstract

When the shallow tunnel is constructed on the slope terrain in the mountains, there are the potential risks such as landslide induced by cutting the slope and the non-compacted backfill material during the construction of the cut-and-cover tunnel. In order to solve these problems, based on a practical engineering, the optimized construction plans of the cut-and-cover tunnel were analyzed by particle flow code (PFC), the key parts of the open-cut construction were identified, and the anti-slide piles countermeasures were proposed. Furthermore, the grouting reinforcement process for the non-compacted backfill material around the shallow tunnel was simulated by PFC, and the variation characteristics of the porosity and grouting pressure were revealed as well. The results are of great value to the similar engineering.

Keywords: Shallow Tunnel, Construction, Landslide, Grouting, Particle Flow Code

1. Introduction

In recent years, with the rapid development of China's economy, the shallow tunnels on the slope terrain in the mountains gradually increased. Since the cover layer of the shallow tunnel is thinner, the open-cut method is usually used to build the shallow tunnel. Then there are the potential risks such as landslide induced by cutting the slope and the non-compacted backfill material during the construction of the cut-and-cover tunnel. So it is very important for safety construction to research on the key technologies of the shallow tunnel [1].

Due to the influence of multiple disturbance of the surrounding rock in period of the shallow tunnel construction, the mechanical behaviors of the cut-and-cover tunnel differ greatly in different construction stages, which often bring great difficulties and potential risks to construction. Therefore, many scholars conducted studies about these problems. For example, Y.M. Wu et al. researched on the distribution and the developing law of displacement and stress of the half-buried tunnel under different conditions by numerical simulation method [2]. Z.L. Shu et al. discussed the stability of the tunnel portal section by the method of half-buried tunnel construction based on design and construction of Qiaowu tunnel [3]. Z. Zhang et al. analyzed the bolt mechanical behavior during the half-dark arch tunnel construction by numerical simulation method [4]. B. Li studied the causes and hazards of unsymmetrical

pressure tunnel through cases collection and statistical analysis, and the influence factors of critical depth of unsymmetrical pressure tunnel were analyzed as well as the principle of control measures [5]. G. Dai et al. identified the construction sequence and support scheme for the portal of the shallow tunnel under unsymmetrical pressure combining with the engineering case of Beileiyuan tunnel [6]. In addition, foreign scholars M. Karakus et al. made a finite element analysis for the twin metro tunnel constructed in Ankara Clay [7]. C.F. Hage et al. conducted numerical analysis of the interaction between twin-tunnels in order to reveal the influence of the relative position and construction procedure [8]. H. Mroueh et al. had completed three-dimensional centrifuge modelling of the effects of twin tunnelling on an existing pile [9]. In order to ensure the stability of the cut-and-cover tunnel, the grouting technique is commonly used to reinforce the surrounding rock of the tunnel. At present, it is still in the trial and exploratory stage for the slurry diffusion process within the soil medium, the effective diffusion range and grouting pressure dissipation, etc [10-12]. H. Zhu et al. analyzed the mechanism of the high pressure and jet grouting for tunnel surrounding soil reinforcement [13]. W. Lv et al. analyzed the deformation and plastic zone of the shallow tunnel based on the mechanism of the grouting reinforcement [14]. F. Sun et al. based on the assumption of Bingham fluid and narrow plate model of grouting diffusion, developed a formula for calculating the diffusion radius in soil considering the time-varying behaviors of grout [15], etc.

Overall, there are still many problems to be studied for the shallow tunnels being built on the slope terrain in the mountains. Therefore, based on a practical engineering, this paper focused on risk assessment on the construction of the

* E-mail address: yjh0571@163.com

cut-and-cover tunnel, and researched on the grouting reinforcement mechanism for the tunnel surrounding soil by using PFC technique.

2. Engineering Background

Taking the highway tunnel on the gravel slope containing clay as an example (Fig. 1), of which the design clear width is 11.0 m and clear height is 5.0 m, and the design driving speed is 80 km/h.

The surrounding rock of the highway tunnel, belonging to class V, is mainly residual soil and fully-strongly weathered tuff. Its stability is poor with the developed rock fracture, where collapse and landslide are easily to occur during open cut construction. The hydro-geological conditions are simple.

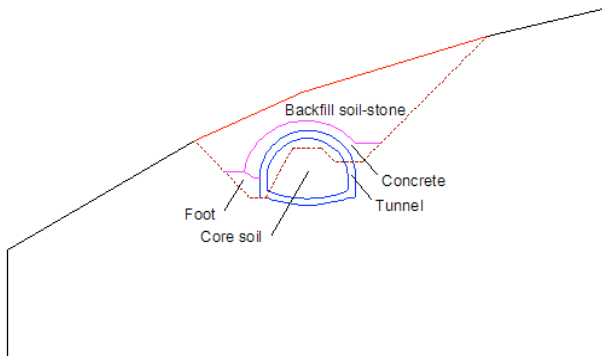


Fig. 1. Cross-sectional schematic of the shallow tunnel

The tunnel would be constructed in the following steps: (1) Cutting the slope by open-cut method; (2) Constructing arch support and the left wall of the tunnel after slope protection; (3) Constructing the anti-slide piles at a distance of the right wall of the tunnel; (4) Backfilling the cover of the tunnel layer by layer; (5) Excavating the reserved core soil and completing the inverted arch and the right wall construction.

3. Mechanics Effect Analysis of Anti-slide Pile

In order to evaluate the mechanics effect on the anti-slide pile, the particle flow code (PFC) was adopted to simulate the both conditions of installing anti-slide pile and no anti-slide pile during the construction of the cut-and-cover tunnel.

3.1 Building Computational Model

In 1971, P.A. Cundall proposed the discrete element method, then Cundall and Strack developed and launched the commercial particle element programs of PFC^{2D} and PFC^{3D} suitable for rock and soil mechanics. PFC is a micro mechanics program developed by using the explicit difference algorithm and the discrete element theory. Based on the internal structure of medium (particles and contacts), PFC can be used to study the macro mechanical characteristics and mechanical response of the micro level of mechanical behavior.

According to the engineering geological conditions and the tunnel construction scheme, the computational model was built based on the typical section as shown in Fig. 2. The bottom and the both side boundaries of the model were fixed, and the top walls were removed after the particles completely generated and the initial stress obtained. Interactions within particles representing the rock and soil mass were described by a contact-bond model, while the connections of particles composing the foundation and arch were simulated with a parallel-bond model to describe the mechanical behavior of tensile, shear and bending moment.

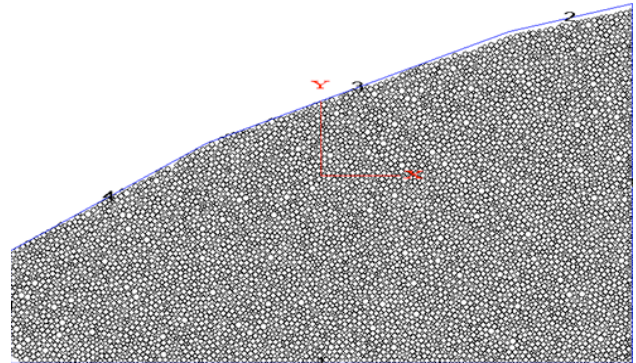


Fig. 2. Particle distribution of the computational

The physical and mechanical parameters adopted in the calculation were listed in Table 1.

Table 1. Physical and mechanical parameters of the computational model

Density (kN/m ³)	Maximum particle (mm)	Minimum particle (mm)	Particle stiffness (MN)	Particle amplification factor	Wall stiffness (MN/m)	Friction coefficient
22.0	250	100	100	1.67	10000	0.30

3.2 Simulation Analysis Scheme

The simulation analysis scheme of the tunnel construction was as follows:

Step 1: Particle generation and initial self-weight stress field calculation. Firstly, the closed walls were created as the model boundaries. Secondly, a certain number of particles of small radius were generated inside the walls with many voids among them, and then the voids were diminished by particle radius expansion. Lastly, the initial stress equilibrium of the particle assemblies was obtained under the self-weight field.

Step 2: Tunnel excavation and protection slope with core soil reserved. Particles representing the excavation area were

deleted following by 20 % increase of friction coefficient and contact-bond strength of the particles that were within the range of right side slope surface to 3.5 meters below according to the engineering analogy method and the engineering experiences, to approximately simulate the bolt reinforcement effect on the slope. Calculation was continued until stress equilibrium to observe the slope deformation due to excavations.

Step 3: Before the construction of left foundation and arch, two cases were considered: with anti-slide pile or not. The foundation and arch were modelled by corresponding shaped particle assemblies with the PFC built-in FISH and Generate command, in which the particle-particle contact was simulated with parallel-bond model in order to play a

supporting role. According to the engineering experiences, in order to reflect the bending effects of the modeling piles and tunnel wall, which were regarded as parallel-bond links.

Step 4: Backfilling rubble concrete at arch foot and soil-stone at vault under the condition of anti-slide pile installation and that of without the pile. Walls were temporarily introduced for generating specific shaped assemblies of backfill particles with the PFC built-in FISH and Generate command, after which the temporary walls were deleted and then calculated to stress equilibrium state.

Step 5: Core soil excavation under the condition of anti-slide pile installation and that of without the pile. The core soil was excavated after the installation of arch and the backfill. As there always was certain time difference between the excavating and supporting, the situation that core soil excavated but not yet supported should be considered by calculating to equilibrium state at this moment, the excavation effect on the right side of the slope could be observed.

Step 6: The inverted arch excavation and backfill with the anti-slide pile installation. The soil particles in tunnel bottom area were deleted and the particles representing inverted arch were generated by using parallel-bond model.

The detail simulation procedures were as follows:

Case 1: Without anti-slide pile

a. Building the slope model; b. Slope excavation; c. Forming the arch foundation of the tunnel; d. Forming the protective arch; e. Backfill to the right foot of the arch; f. Backfill to the left and roof of the arch; g. Backfill to the right and roof of the arch; h. Excavation reserved core soil.

Case 2: With anti-slide pile

a. Building the slope model; b. Slope excavation; c. Setting anti-slide pile; d. Forming the arch foundation of the tunnel; e. Forming the protective arch; f. Backfill to the right foot of the arch; g. Backfill to the left and roof of the arch; h. Backfill to the right and roof of the arch; i. Excavation reserved core soil; j. Floor excavation and tunnel support.

3.3 Mechanics Effect Analysis of the Anti-slide Pile During the Tunnel Construction

Fig. 3 shows the displacement vector field of the slope after open-cut, from which it can be seen that two slopes were formed at both sides of the tunnel location after 1:1 step-slope excavation, with a low left slope and the right slope at 17 meters high. As the rock and soil of the interested area was mainly loose gravel with clay, the large displacement toward the free side appeared at the right slope after open cut and part of which showed a sliding trend. The left low slope shaped to the free side too but the displacement was lower.

Figs. 4 and 5 show the construction of tunnel foundation and supporting arch with anti-slide pile and without, respectively.

Figs. 6 and 7 show the backfill construction at tunnel vault with anti-slide pile and without, respectively.

From Figs. 8 and 9 it can be seen that the maximum displacement of the right slope due to core soil excavation was 381 mm under the installation of anti-slide pile, which was smaller than that of without anti-slide pile (852 mm). Therefore the anti-slide pile was necessary for reducing the slide hazard due to core soil excavation.

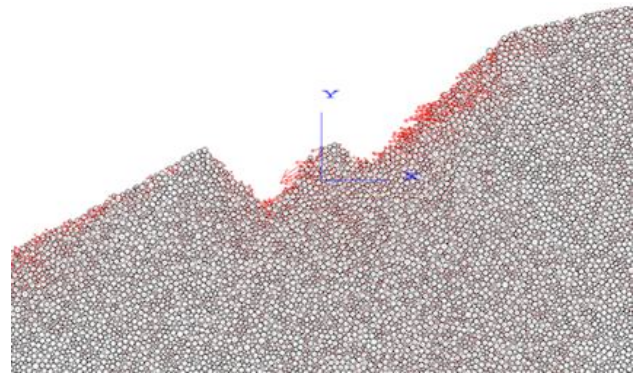


Fig. 3. Displacement vector field after open-cut excavation

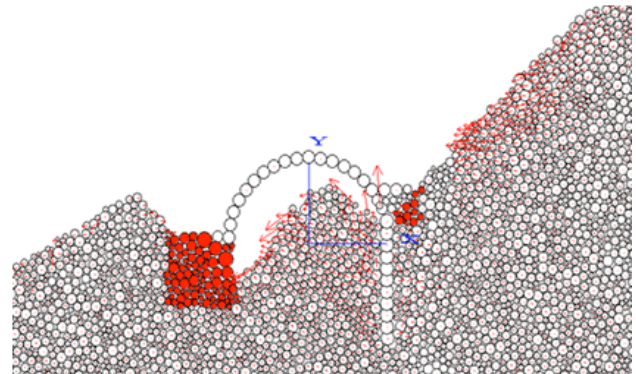


Fig. 4. Tunnel arch construction with anti-slide pile

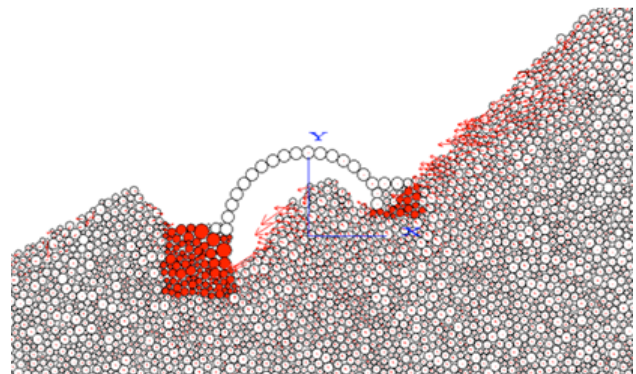


Fig. 5. Tunnel arch construction without anti-slide pile

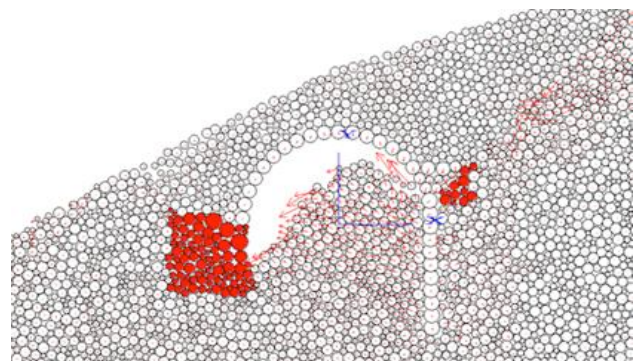


Fig. 6. Backfill soil-stone with anti-slide pile

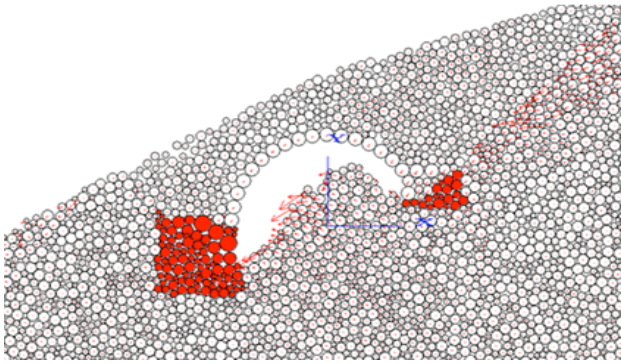
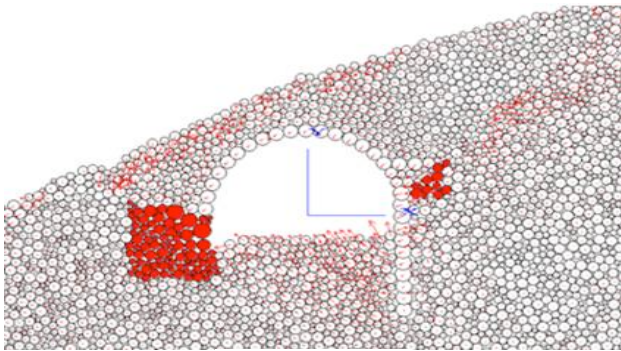
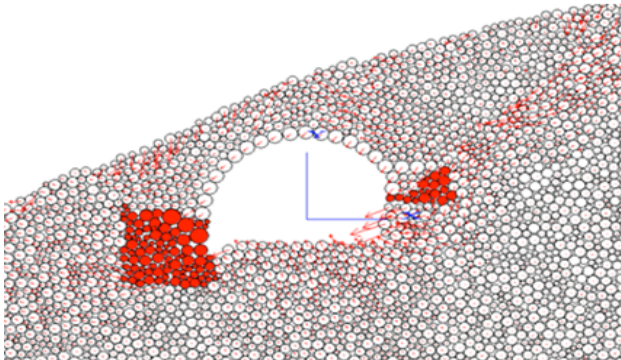


Fig. 7. Backfill soil-stone without anti-slide pile



Displacement
Maximum = 3.809e-001

Fig. 8. Displacement vector field with anti-slide pile



Displacement
Maximum = 8.522e-001

Fig. 9. Displacement vector field without anti-slide pile

Fig. 10 shows the completed tunnel project under the installation of anti-slide pile. The scheme with anti-slide pile was adopted in field construction as shown in Fig. 11.

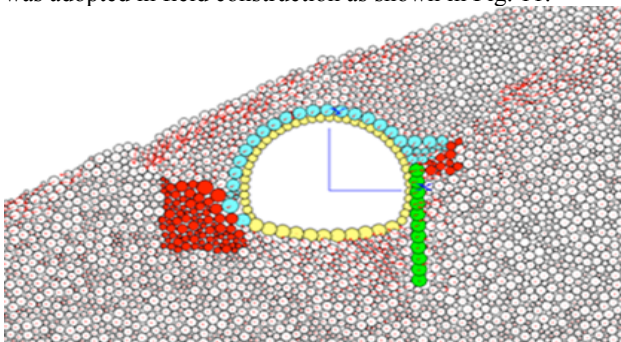


Fig. 10. Displacement vector field of the completed tunnel



Fig. 11. Setting anti-slide pile at construction site

4. Fracturing Grouting Liquid-solid Coupling Analysis in the Surrounding Rock of Tunnel

4.1 Liquid-solid Coupling in PFC

The void geometry in an assembly of circular particles in PFC is regarded as a network structure of identical dots linked by pipe between two adjacent domains.

As far as the fluid is concerned, the pipe is equivalent to a parallel-plate channel, with length L , aperture a and unit depth (in the out-of-plane dimension). The flow rate (volume per unit time) in a pipe is given by:

$$q = ka^3 \frac{P_2 - P_1}{L} \quad (1)$$

Where k is a conductivity factor and $P_2 - P_1$ is the pressure difference between the two adjacent domains. The sign convention is such that a positive pressure difference produces a positive flow from domain 2 to domain 1.

(1) When the compressive force is taken as positive, the aperture a satisfied the following equation:

$$a = \frac{a_0 F_0}{F + F_0} \quad (2)$$

Where a_0 is the residual aperture for zero normal force, F_0 is the value of normal force, F is the value of normal force at which the aperture decreases to $a_0/2$.

(2) When the normal force is tensile (intact bond) or it is zero, then the aperture a is simply equal to:

$$a = a_0 + mg \quad (3)$$

Where m is a dimensionless multiplier, g is the normal distance between the surfaces of the two particles.

Each domain receives the flows from the surrounding pipes: $\sum q$. In one timestep Δt , the increase in fluid pressure is given by the following equation, assuming that inflow is taken as positive.

$$\Delta P = \frac{K_f}{V_d} \left(\sum q \Delta t - \Delta V_d \right) \quad (4)$$

Where ΔP is the increment fluid pressure, K_f is the fluid bulk modulus and V_d is the apparent volume of the domain.

In a word, there are three forms of coupling between the fluid and the solid particles in PFC as follows: (1) Changes in aperture are caused by contact opening and closing, or changes in contact force; (2) Mechanical changes in domain

volumes cause changes in domain pressures; (3) Domain pressure exerts tractions on the enclosing particles.

4.2 Building Computational Model

The model considered was a range of 10 m × 10 m (width × height) in which the center was installed a grouting hole with a drainage area of radius 0.1 m and a grouting pressure 1.5 MPa (Fig. 12).

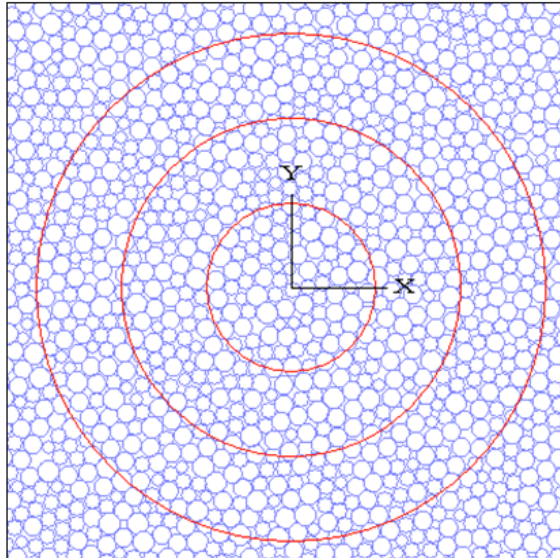


Fig. 12. Particle distribution of the model

Table 2. Physics and mechanics parameters of the particle model

Density (kN/m ³)	Maximum particle (mm)	Minimum particle (mm)	Particle stiffness (MN)	Particle amplification factor	Porosity	Friction coefficient
20.0	120	80	100	1.60	0.15	0.20

Table 3. Parameters used in fracturing grouting test

Grouting pressure (MPa)	Permeability coefficient (m/sec)	Aperture for zero normal force (mm)	Normal force when aperture decreases to half aperture (Pa)
1.5	0.65	1.0	5000

4.3 Simulation Analysis Scheme

The simulation analysis scheme was as follows:

Step 1: The computational model was built and calculated to stress equilibrium state under soil self-weight, then the displacements of particles were reset to zero.

Step 2: Based on the above step, the initial equilibrium of fluid-solid coupling was executed and after which the displacements of particles were reset to zero.

Step 3: Under the given grouting pressure, the fracturing grouting test was simulated with fluid-solid coupling calculation.

4.4 Grouting Effect Analysis in the Surrounding Rock of Tunnel

It could be seen from Fig. 13 that the grouting pressure (blue) spread from the center grouting hole to the surrounding soil and got smaller under the given grouting pressure of 1.5 MPa. The compression (red) and tension (black) cracks appeared in the surrounding soil from the near to the distant. Most cracks occurred within a radius of 1.0 m and very few cracks could be found outside a radius of 2.0 m, which

In order to analyze the variations of the porosity and grouting pressure in the surrounding soil around the grouting hole, three measurement circles were set up with radii of 1.0 m, 2.0 m and 3.0 m, respectively. The computational model built by PFC is shown in Fig. 12.

The physics and mechanics parameters used in the model are listed in Table 2 and Table 3.

meant that the main controlling scope of grouting fracture was within a radius of 2.0 m.

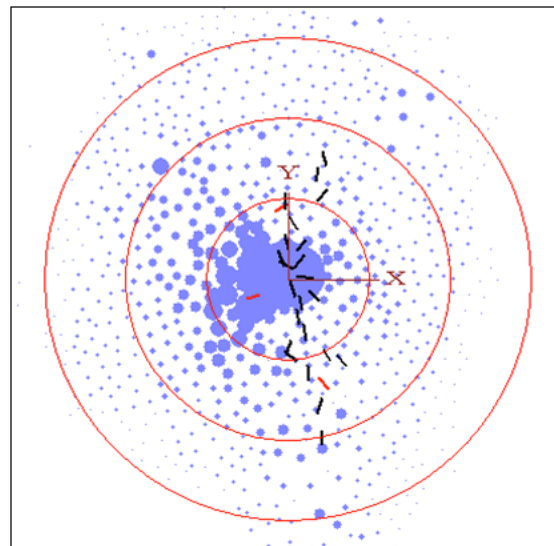


Fig. 13. Map of grouting pressure and fracture propagation

Figs. 14 and 15 show the curves of porosity and compressive stress in the surrounding soil of the grouting hole, respectively, under different measurement ranges. The porosity variation in the surrounding soil was on the whole spreading inside-out from large to small (Fig. 14) during the grouting test. In the initial stage, the soil porosity within the 2.0 m radius circle started lower than that within the 3.0 m radius circle and ended higher, which meant the grouting process experienced a gradual development of near fracturing and distant compacting. The particle stress in the soil around the grouting hole was also spreading inside-out from large to small (Fig. 15) and experienced the complicated variation of tension and compress during the grouting test.

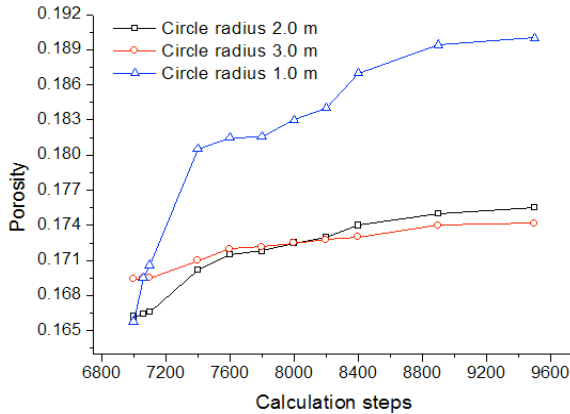


Fig. 14. Porosity variation curves of the grouting hole

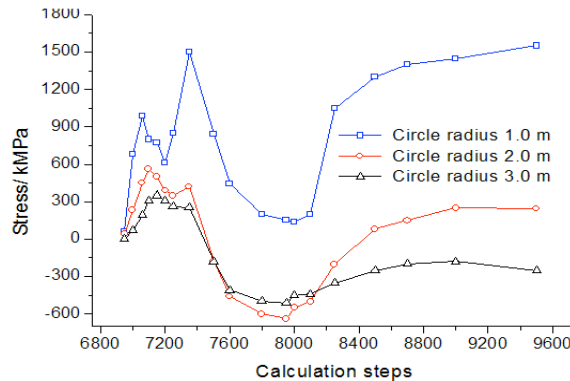


Fig. 15. Particle stress variation around the grouting hole

5. Conclusion

For the shallow tunnel construction on the slope in mountains, the nonlinear mechanical behavior under loading and unloading conditions (e.g. excavation and backfill construction) can be modelled by PFC technique and the particle displacement trends can be displayed graphically. The results showed the construction scheme with anti-slide pile could effectively control the landslide and reduce risks during the core soil excavation, which was of certain reference value to similar engineering.

The process of crack generation, development and extension during fracturing grouting process can be simulated by using PFC technique. The grout diffusion, soil compaction and fracturing effect during the grouting process were analyzed based on a practical engineering, which is of great meaning of theoretical and practical in discussing and building the connections between micro variation of physical and mechanical parameters and the macro mechanical response.

Acknowledgments

This work was financially supported by the National Natural Science Foundation of China (51474188; 51074140; 51310105020), the Natural Science Foundation of Hebei Province of China (E2014203012) and Program for Taihang Scholars, all these are gratefully acknowledged.

References

1. Yang J.-H., Wang S.-R., Li C.-L. and Li Y., "Disturbance deformation effect on the existing tunnel of asymmetric tunnels with small spacing", *Disaster Advances*, 6 (13), 2013, pp. 269-277.
2. Wu Y.-M., Wang F., Zou Z.-M. and Lu K.-C., "Mechanical character analysis and in-situ monitoring for portal section of half-buried tunnel", *Chinese Journal of Rock Mechanics and Engineering*, 27 (S1), 2008, pp. 2873-2882. (in Chinese)
3. Shu Z.-L., Xu D.-X., Xu K., Liu X.-R. and Li S., "Study on construction of portal section of half-buried tunnel", *Chinese Journal of Underground Space and Engineering*, 6 (5), 2010, pp. 1060-1064. (in Chinese)
4. Zhang Z., Mo H.-J. and Tan Y., "Analysis of the bolt mechanical behavior during the half-dark arch tunnel construction", *Sichuan Architecture*, 30 (3), 2010, pp. 178-181. (in Chinese)
5. Li B., "Study on disease characteristics of unsymmetrical pressure tunnel and its control measures", *Journal of Railway Science and Engineering*, 8 (6), 2011, pp. 59-63. (in Chinese)
6. Dai G. and Zhang R.-G., "On portal construction technique of Beileiyuan shallow tunnel under unsymmetrical pressure", *Shanxi Architecture*, 39 (15), 2013, pp. 174-176. (in Chinese)
7. Karakus M., Ozsan A. and Basarir H., "Finite element analysis for the twin metro tunnel constructed in Ankara Clay, Turkey", *Bulletin of Engineering Geology and the Environment*, 66 (1), 2007, pp. 71-79.
8. Hage C.-F. and Shahrour I., "Numerical analysis of the interaction between twin-tunnels: Influence of the relative position and construction procedure", *Tunnelling and Underground Space Technology*, 23 (2), 2008, pp. 210-214.
9. Mroueh H. and Shahrour I., "Three-dimensional finite element analysis of the interaction between tunneling and pile foundations", *International Journal for Numerical and Analytical Methods in Geomechanics*, 26 (3), 2002, pp. 217-230.
10. Duan B.-F. and Li L., "Grouting reinforcement technique for subsurface excavation of group metro tunnels construction in complex environment", *Disaster Advances*, 5 (4), 2012, pp. 105-109.
11. Croce P. and Flora A., "Analysis of single-fluid jet grouting", *Géotechnique*, 50 (6), 2000, pp. 739-748.

12. Tu J.-W., Tang A.-P., Liu Y.-J and Liu K.-T., "Effect of Surcharge on the Stability of Rock Slope under Complex Conditions", *Journal of Engineering Science and Technology Review*, 6 (2), 2013, pp. 173-178.
13. Zhu H. and Du J.-H., "Theory analysis and engineering application of tunnel surrounding rock grouting", *Journal of Shenyang Jianzhu University (Natural Science)*, 28 (3), 2012, pp. 498-500. (in Chinese)
14. Lv W. and Ji X.-M., "Numerical simulation of double liquid grouting reinforcement for shallow-buried tunnel", *Journal of Shenyang Jianzhu University (Natural Science)*, 35 (2), 2012, pp. 225-229. (in Chinese)
15. Sun F., Zhang D.-L. and Chen T.-L., "Fracture grouting mechanism in tunnels based on time-dependent behaviors of grout", *Chinese Journal of Geotechnical Engineering*, 33 (1), 2011, pp. 88-93. (in Chinese)